Electronic Supplementary Material (ESI) for ChemComm.

Electronic Supporting information

Graphitic carbon nitride catalysed photoacetalization of aldehyde/ketones under ambient conditions

M. Abdullah Khan, Ivo F. Teixeira, Molly M. J. Li, Yusuke Koito and S. C. Edman Tsang*

Experimental

g-C_3N_4 used in this study was synthesized following the method described in previous reports.[1,2]

Characterization

X-ray diffractions (XRD) patterns were measured on PANanlytical X'Pert Pro diffractometer operating in Bragg–Brentano focusing geometry and using Cu Ka radiation (k = 1.5418 Å) from a generator operating at 40 kV and 40 mA. Steady-state and time-resolved Photoluminescence (PL) measurements were acquired using a time-correlated single photon counting (TCSPC) setup (FluoTime300, PicoQuant GmbH). The samples were excited using a 405 nm laser pulsed at frequencies between 0.3-10 MHz. The PL was collected using a high resolution monochromator and hybrid photomultiplier detector assembly (PMA Hybrid 40, PicoQuant GmbH).[3,4] Transmission electron microscopy (TEM) images were recorded on JEOL 2010 equipped with a high-resolution pole piece running at 200 kV accelerating voltage. SEM images were taken on JEOL 6500F FEG SEM with voltage of 5KV and working distance of 10mm. XPS measurements were done using a Thermo Scientific K-Alpha XPS instrument equipped with a microfocussed monochromated Al X-ray source. The source was operated at 12 keV and a 400 micron spot size was used. The analyser operates at a constant analyser energy (CAE) of 200 eV for survey scans and 50eV for detailed scans. Charge neutralization was applied using a combined low energy / ion flood source. The data acquisition was performed with Thermo Scientifics Avantage software and data analysis was performed with Igor pro along with XPS fit procedure. The Curve fitting of spectra was done using Gaussian-Lorentzia line shape after performing the shrilly background corrections. The Fourier transform infrared (FTIR) was performed on a Nicolet 6700 FT-IR spectrometer with a MCT detector cooled using liquid nitrogen. The obtained spectra are averaging the 128 scans with 4 cm^{-1} resolution. Solid-state Cross-Polarization Magic Angle Spinning Carbon-13 (^{13}C CPMAS) NMR spectra was collected on Bruker Avance III HD 400MHz Solid state NMR. UV/Vis absorbance spectra were recorded at room temperature with UV-vis spectrometer (Lambda 750S, Perkin Elmer) with potassium bromide as reference.

Photocatalytic tests

The photoacetalization reactions were carried out in an outer irradiation-type photoreactor (Pyrex glass) using 300 W Xenon lamp. The distance between irradiation source and photoreactor was kept where the light intensity was 1.5 AM and the wavelength of the incident light was controlled by using 420 nm cut off filter. Approximately 0.025 g of the photocatalysts was dispersed by a magnetic stirrer in 5 mL of methanol and 1mM of substrate was added. The suspension was purged with O_2 for 5 min and irradiated with visible light. Magnetic stirring (400 rpm) was used during the experiment to ensure homogeneity of the suspension and to avoid sedimentation. The reaction products were identified and quantified by GC-MS (Agilent 6890 and Agilent MSD 5973 (N)).

Controlled Experiments

Control experiments were performed as specified in order to better understand the mechanism. The reaction in the absence of O_2 was carried out under the same condition of other experiments, however, O_2 was replaced by argon gas (Table S1/Ar). The reaction was also tested by adding 0.5 mL of 30wt% H_2O_2 as oxidant instead of O_2 (Table S1/H_2O_2). In order to verify the role of superoxide radicals in the reaction, 100 mg of benzoquinone, a superoxide radical scavenger, was added into the reaction system (Table S1/BQ).

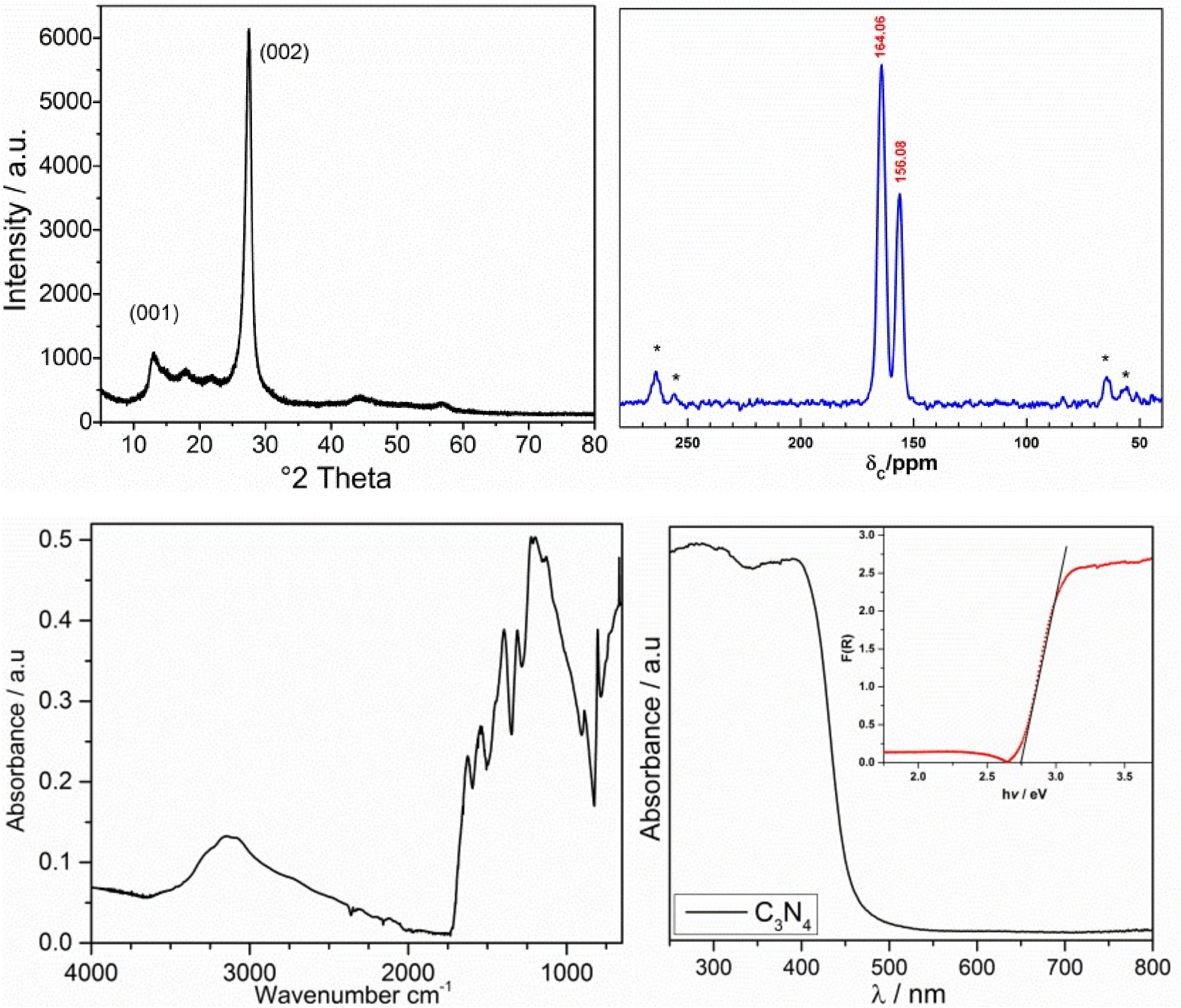

Figure S1. XRD patterns (top left), solid-state ^{13}C MAS NMR (* spinning side bands in ^{13}C spectra, top right), FTIR profile (bottom left) and UV-vis absorption spectra (bottom right) with the inset showing a band gap of 2.7eV of graphitic carbon nitride powder.

XRD patterns confirmed the synthesized material was graphitic carbon nitride. They showed three distinct diffraction peaks which were located at 2θ of 13.1°, 27.2°, 44.2°, respectively. The 13.04° (100) peak was due to interlayer stacking of conjugated aromatic systems; 27.2° (002) to the in-plane structural packing motifs and 44.2 (200) to triazine-based graphitic CN, respectively as similar to previous reports (Fig. S1).[1,2]

In FTIR spectrum, typical bands at around 800-812 cm^{-1} corresponded to breathing mode of tri-s-triazine/s-triazine ring sextant out of plan bending, linked by -NH- groups at 1200-1400 cm^{-1} and 1200-1630 cm^{-1} of ν (C-NH-C) and ν (C=N, C=C) stretching vibrations in fingerprint region. All features were of typical carbon nitride material (Fig. S1).

The solid state ^{13}C MAS NMR signals at approximately 155 and 164 ppm were related to formation of poly(tri-s-triazine) motifs of melem. The side bands with asterisk indicated the spinning side bands of the ^{13}C spectra (Fig. S1).

The UV-vis spectra also showed a typical optical absorption of carbon nitride around 460 nm and the inset showing the band gap E_g = 2.7 which was calculated using equation $\alpha h\nu = A(h\nu - E_g)^n$, where α, ν, and A are the absorption coefficient (Kubelka-Munk function), light frequency, and a constant 1, respectively. (Fig. S1).

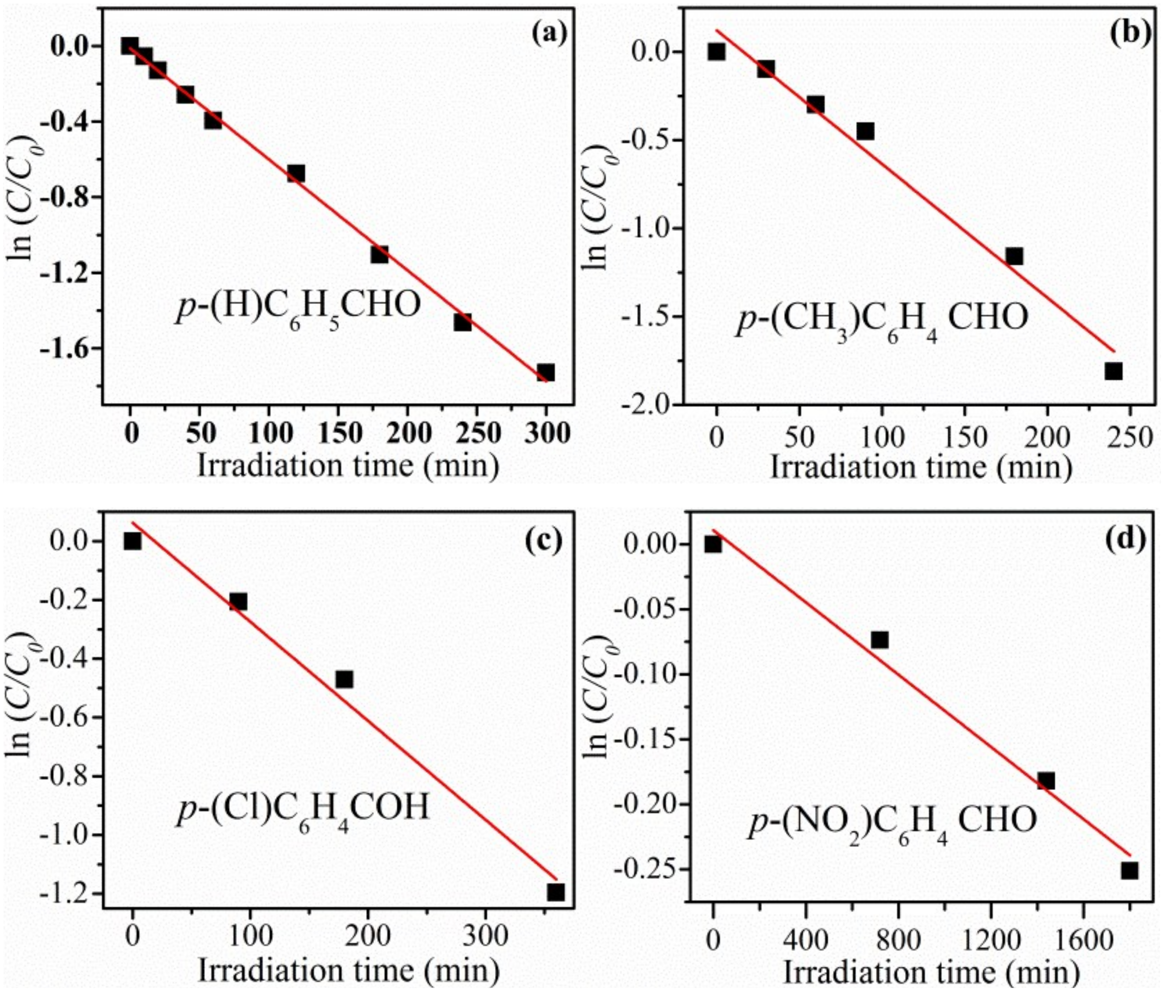

Figure S2. Plots of ln(C/C_0) vs time for benzaldehyde with (a) H, (b) CH_3 (c) Cl (d) NO_2 groups.

Table S1: Photocatalytic rate constants (*k*-values) for H, CH_3, Cl, and NO_2 substituted benzaldehyde

	***k*-value [min^{-1}]**	**Adj. *R*-Square**
p-(H)C_6H_4 CHO	-0.00587 ± 1.12×10^{-4}	0.99715
p-(CH_3)C_6H_4 CHO	-0.00758 ± 5.31×10^{-4}	0.97588
p-(Cl)C_6H_4 CHO	-0.00337 ± 2.9 ×10^{-4}	0.97717
p-(NO_2)C_6H_4 CHO	-1.38839 ×10^{-4} ± 1.1 ×10^{-5}	0.97798

Table S2. Control experiments under different conditions specified below

Entry	Substrate	Time / h	Conversion %	Selectivity / %
				Acetal
*Ar	Benzaldehyde	48	35.15	10.18
+H_2O_2	Benzaldehyde	6	71.2	42.30
‡BQ	Benzaldehyde	6	98.30	99.41

* Reaction purged during 5 min with argon; + Reaction with addition of 0.5 mL of H_2O_2; ‡ Reaction carried out in the presence of 100mg benzoquinone (BQ);

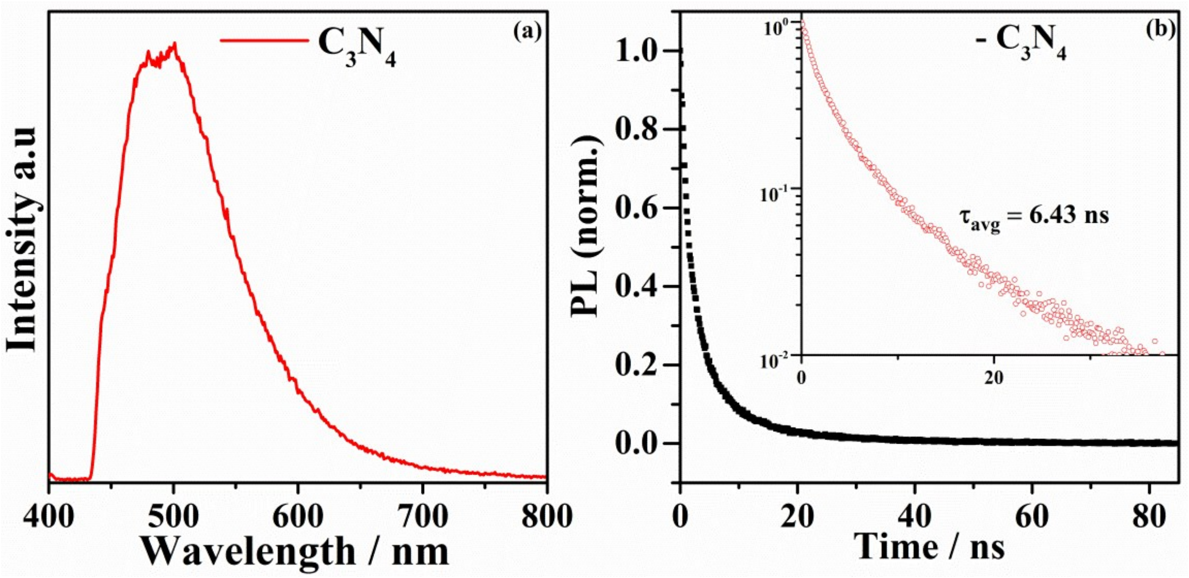

Figure S3a. Steady state photo-luminescence of graphitic carbon nitride powder; **b**. Time-resolved photoluminescence of g-C_3N_4 film excited by 405 nm laser pulsed at frequencies of 32 MHZ.

The steady-state photoluminescence (PL) of graphitic carbon nitride recorded at room temperature is shown in Figure S3a. The observed features near 450 nm corresponded to π-π* transitions, whereas the emission around 500 nm was associated to n-π* manifold of conjugated heptazine units of CN. These results are consistent with previous findings.[5,6] Further in the Figure S3b, the PL decay of the pristine carbon nitride exhibited an average decay time constant of τ_{vg} = 6.43ns which is sufficiently long enough to activate aldehyde/ketones molecules by the transient charged surfaces.

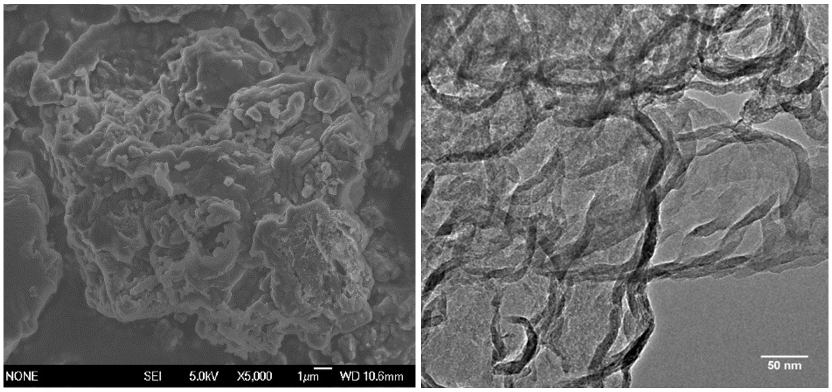

Figure S4. SEM and HRTEM image of Carbon nitride.

TEM and SEM images of pristine C_3N_4 samples showed a typical aggregated, large size, flat surface structure (Fig. S4).

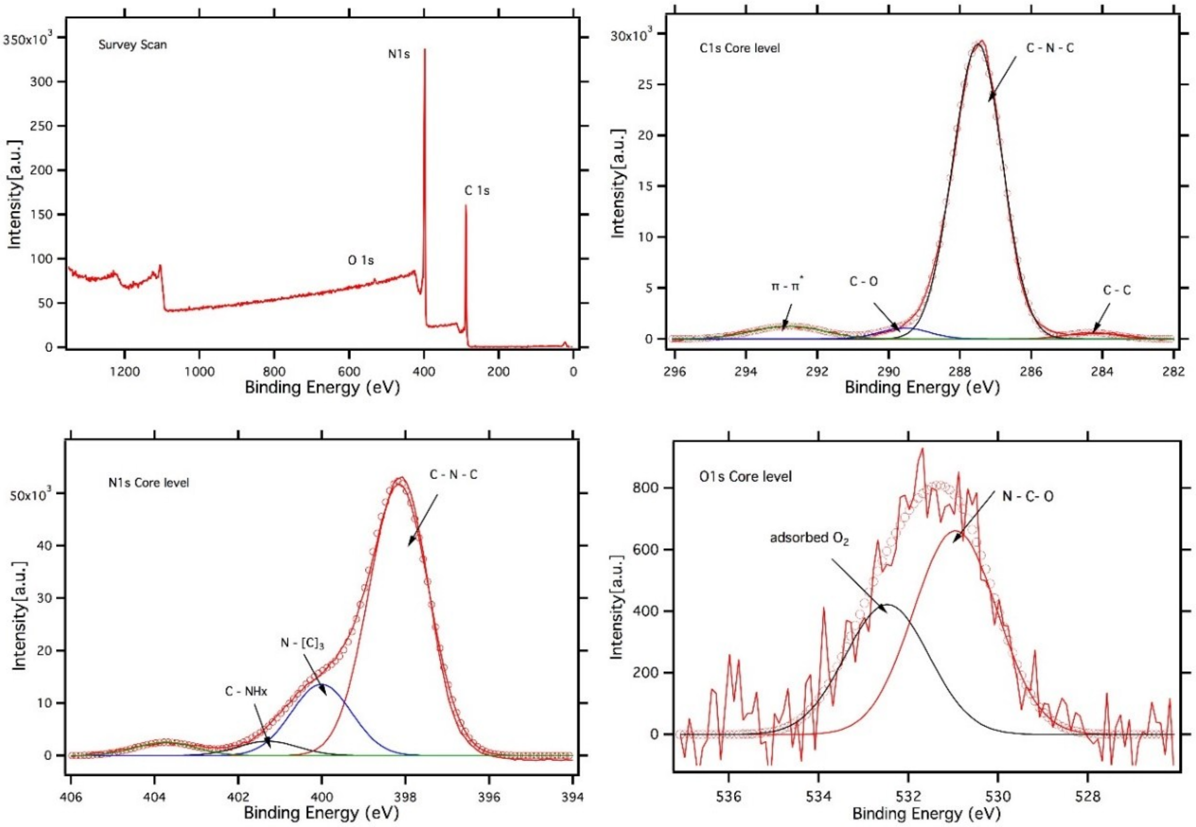

Figure S5. XPS spectra of carbon nitride (a) survey (b) C 1s (c) N 1s (d) O 1s synthesized from thermal polycondensation of dicyandiamide (DCDA).

X-ray photoelectron spectroscopy (XPS) showed C 1s and N 1s peaks along with residual O 1s peak (Fig. S5) The latter was probably due to surface adsorbed oxygen.[7] C 1s spectra clearly showed the C-C, predominant C-N-C, and traces of C-O bonding at 284.5, 287.8 and 289.1 eV, respectively. The N 1s spectra showed four signals at core levels at 398.3, 400.1, 401.2 and 404 eV, which were attributed to sp^2 C-N-C, (atomic % of bond 69.3) sp^3 H-N-[C$_3$] (14.8), C-NH$_x$ (12.2) and terminal nitrate groups with charging effects or π excitations.[7,8] A traces of adsorbed oxygen at 532.9 eV and N-C-O at 530.8 were also observed.

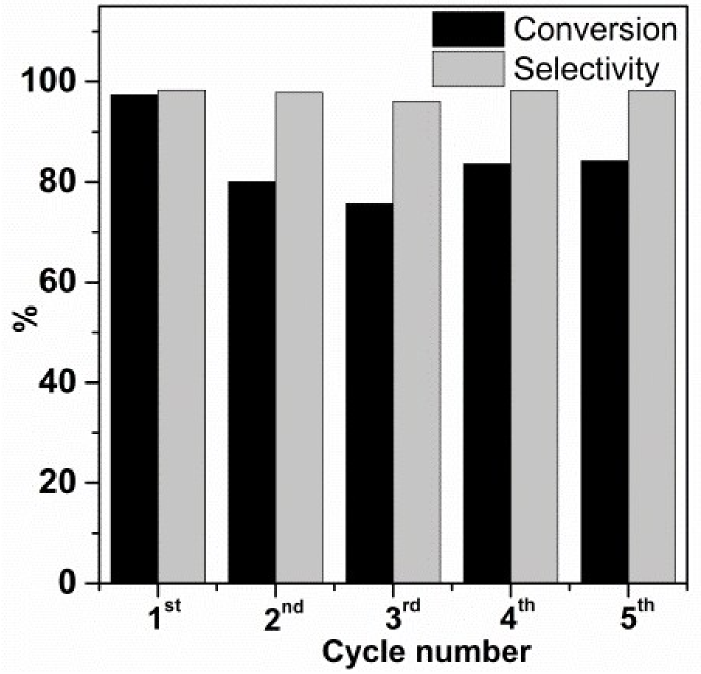

Fig. S6 A stability test for photoacetalization of g-C_3N_4

Stability of the g-C_3N_4 powder catalyst was evaluated by repeated catalytic tests with powder separation from reaction mixture (centrifugation), drying (overnight at 80 °C) and re-charging into new batch of substrates intermittently. As seen from Figure S6, the catalyst exhibits repeatable catalytic performance when re-employed with new substrate mixture for five consecutive cycles. Only a small appreciable loss of activity was noticed after the first cycle due to the loss of the most superfine particles during centrifugation whereas negligible loss of activity was then recorded in subsequent cycles. In addition, no difference in activity was found disregard whether the spent catalyst was received with or without treatment at 200 °C. This suggests that the working catalyst had not suffered from any major surface fouling. The result clearly suggests that g-C_3N_4 can be re-used without any vigorous catalyst regeneration after the photoacetalization.

Scheme S1. Proposed transition states and pathways from hemiacetal to acetal formation.

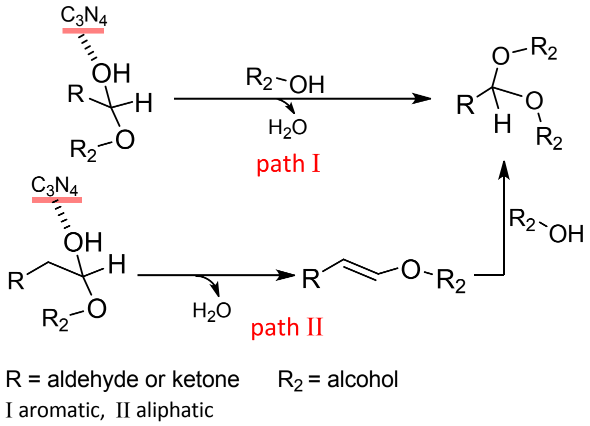

Remarks during revisions of this paper

As far as we are aware there has been no work in open literature on the catalytic photoacetalization using visible light although Liu and co-workers[9] have recently applied nano-TiO_2 as photocatalyst for this reaction. However, the scope of their substrates was narrower than our present work, and UV light was used instead.

Regarding the kinetic catalytic analysis of the g-C_3N_4 catalyst, a first order dependence on substrate concentration was obtained under our excess substrate to catalyst mass ratios (Fig. S2). It is noted that the study of catalyst concentration on exact reaction rate have not yet carried due to the concern of its dispersion in solution. At present, our solid catalyst particles were not well dispersed in solution despite the vigorous stirring during reaction. We are working to reduce the size of the g-C_3N_4 catalyst to colloid nanoparticles before this kinetic study can be taken place.

References

[1] X. Wang, K. Maeda, A. Thomas, K. Takanabe, G. Xin, J. M. Carlsson, K. Domen, M. Antonietti, *Nat. Mater.* **2009**, *8*, 76–80.

[2] F. Su, S. C. Mathew, G. Lipner, X. Fu, M. Antonietti, S. Blechert, X. Wang, *J. Am. Chem. Soc.* **2010**, *132*, 16299–16301.

[3] C. Ma, C. T.-L. Chan, W.-M. Kwok, C.-M. Che, *Chem. Sci.* **2012**, *3*, 1883.

[4] S. D. Stranks, G. E. Eperon, G. Grancini, C. Menelaou, M. J. P. Alcocer, T. Leijtens, L. M. Herz, A. Petrozza, H. J. Snaith, *Science (80-.).* **2013**, *342*, 341–345.

[5] A. B. Jorge, D. J. Martin, M. T. S. Dhanoa, A. S. Rahman, N. Makwana, J. Tang, A. Sella, F. Corà, S. Firth, J. A. Darr, et al., *J. Phys. Chem. C* **2013**, *117*, 7178–7185.

[6] Y. Zhang, Q. Pan, G. Chai, M. Liang, G. Dong, Q. Zhang, J. Qiu, *Sci. Rep.* **2013**, *3*, 1943.

[7] D. J. Martin, K. Qiu, S. A. Shevlin, A. D. Handoko, X. Chen, Z. Guo, J. Tang, *Angew. Chem. Int. Ed.* **2014**, *53*, 9240–5.

[8] A. Thomas, A. Fischer, F. Goettmann, M. Antonietti, J.-O. Müller, R. Schlögl, J. M. Carlsson, *J. Mater. Chem.* **2008**, *18*, 4893.

[9] M. Ye, G. Zhou, B. Li, J. Liu, Scientia Sinica Chimica 43 (2013) 551-557.